World Academy of Science, Engineering and Technology
International Journal of Mechanical and Mechatronics Engineering
Vol:13, No:7, 2019

Corrosion Analysis and Interfacial Characterization of Al – Steel Metal Inert Gas Weld - Braze Dissimilar Joints by Micro Area X-Ray Diffraction Technique

S. S. Sravanthi, Swati Ghosh Acharyya

***Abstract*—**Automotive light weighting is of major prominence in the current times due to its contribution in improved fuel economy and reduced environmental pollution. Various arc welding technologies are being employed in the production of automobile components with reduced weight. The present study is of practical importance since it involves preferential substitution of Zinc coated mild steel with a light weight alloy such as 6061 Aluminium by means of Gas Metal Arc Welding (GMAW) – Brazing technique at different processing parameters. However, the fabricated joints have shown the generation of Al – Fe layer at the interfacial regions which was confirmed by the Scanning Electron Microscope and Energy Dispersion Spectroscopy. These Al-Fe compounds not only affect the mechanical strength, but also predominantly deteriorate the corrosion resistance of the joints. Hence, it is essential to understand the phases formed in this layer and their crystal structure. Micro area X - ray diffraction technique has been exclusively used for this study. Moreover, the crevice corrosion analysis at the joint interfaces was done by exposing the joints to 5 wt.% $FeCl_3$ solution at regular time intervals as per ASTM G 48-03. The joints have shown a decreased crevice corrosion resistance with increased heat intensity. Inner surfaces of welds have shown severe oxide cracking and a remarkable weight loss when exposed to concentrated $FeCl_3$. The weight loss was enhanced with decreased filler wire feed rate and increased heat intensity.

***Keywords*—**Automobiles, welding, corrosion, lap joints, Micro XRD.

I. Introduction

IN the current times, the steel in automobile components are undergoing preferential substitution with light weighted materials such as aluminium and its alloys. Various joining technologies are being adopted for the fabrication of the aluminium-steel fusion hybrid blanks [1]-[3]. Fig. 1 shows the preferential substitution of steel with aluminium in the subframe of the car body by friction stir welding. However, Al-steel welding leads to the Al-Fe intermetallic generation at the interfaces of the fabricated welds due to a wide mismatch in their metallurgical properties [4], [5]. An extensive research is going on in understanding the effect of the intermetallics on the corrosion behaviour and mechanical performance of these welds [6]-[8]. In addition to this, it is known from the literature that high strength welds of Al-steel can be fabricated in lap joint configuration [9], [10]. However, this configuration generates an inevitable interfacial gap that leads to crevice corrosion through the weld interfaces. Therefore, in addition to understanding the crystal structure of the intermetallic phases generated at the weld interfaces, it is essential to study the impact of lap joint configuration of dissimilar welds on their crevice corrosion resistance. The authors have previously reported the intergranular corrosion resistance of aluminium – steel welds in highly corrosive medium [11], [12], [21]. Hence, in the present work, the authors make a systematic effort in understanding the effect of varying heat input and the lap joint configuration of 6061 Al – Mild steel dissimilar welds on their crevice corrosion behaviour.

S. S. Sravanthi and Swati Ghosh Acharyya are with the School of Engineering Sciences and Technology, University of Hyderabad, India 500046.

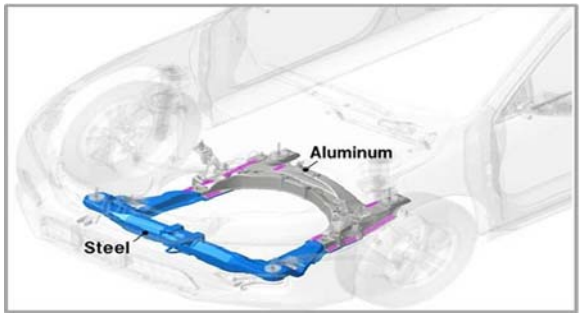

Fig. 1 Substitution of steel with Aluminium in the centre frame of a car body

II. Experimental Procedure

A. Materials

The 6061 Al alloy used for the experiment was T6 heat treated for which a solution treatment was given at ~ 525 ºC and was then subjected to aging for one hour. It was then sectioned to 75 mm x 75 mm x 1.5 mm dimensions and was posotioned on zinc coated mild steel plate of dimensions 75 mm x 75 mm x 1.5 mm for welding after fixing it tightly. The Al - 5% Si alloy of diameter 1.25 mm was used as filler material since Si of the alloy is known for fludity enhancement and increasing crack resistance of the alloy [13]. The details of the chemical composition of alloys are given in Table I.

B. Welding Methods

The weld fabrication was done in Argon atmosphere at a flow rate of 20 $L.min^{-1}$ fixed for all the welds. The current and voltage used for welding were fixed from the initial literature survey [14]-[16]. The GMAW-brazing procedure involves a

quick movement of the pulsed arc along the corner of 6061 aluminium plate which was placed over zinc coated steel plate. This is followed by brazing of Al - 5% Sifiller, by keeping the brazing torch at 80° through the corner of 6061 aluminium plate. The welding parameters viz., filler feed rate and weld speed were varied during the process and sound GMAW-braze joints were fabricated. The details of the welding parameters and heat input are given in Table II.

TABLE I
MATERIALS USED - ELEMENTAL COMPOSITION

Materials	Weight (%)								
	Si	Mg	Cu	C	Mn	P	S	Fe	Al
6061 Al	0.5	1.08	0.2	--	0.07	--	--	0.4	Bal
Al-5%Si filler	5.01	0.4	0.28	--	0.11	--	--	0.5	Bal
Mild steel	0.2	--	--	0.09	0.01	0.007	0.006	Bal	--

TABLE II
WELDING DETAILS OF MIG-BRAZE SAMPLES

Sample ID	Weld speed (m/min)	Wire feed rate (m/min)	Current (A)	Voltage (V)	Heat Input (J/mm)
B1	0.9	4.5	65	15.5	80.9
B2	0.9	5.5	75	16.5	90.1
B3	1.0	5.0	70	16	85.3

C. Electron Microscopy

To understand the microstructures at the weld interfaces, the samples were seen under scanning electron microscope along the cross section at avoltage of 20 kV. The elemental composition was determined using Energy Dispersion Spectroscopy (EDS). Prior to the microstructural observation, the samples were cut through the cross-sectional area to 20 mm x 5 mm dimensions and were thoroughly cleaned. They were then polished using SiC papers of size 550, 620, 880, 1200 and fine papers 1, 2 and 3. The samples were then subjected to disc polishing using alumina powder of particle size 0.3 µm.

D. Micro-Area X Ray Diffraction

The crystal structure of the intermetallics generated at the interface and their presence at the bead – steel interface was confirmed by micro area XRD. For this purpose, a high intensity X ray beam of size 10 µm was directed onto the intermetallic region of the welds of ~ 2.5 mm x 6.5 mm dimensions through a micro-focussing source [17].

E. Corrosion Analysis

The crevice corrosion behaviour of the present lap joints was determined by conducting the test as per ASTM G 48-03 [18]. The samples were exposed to $FeCl_3.6H_2O$solution periodically and the weight loss was determined at 1st, 3rd and 6th hour of exposure. The welds were broken to visually examine the inner surfaces as shown in Fig. 1. This is followed by microstructural examination of the inner surfaces of welds at 6th hour of immersion in $FeCl_3$.

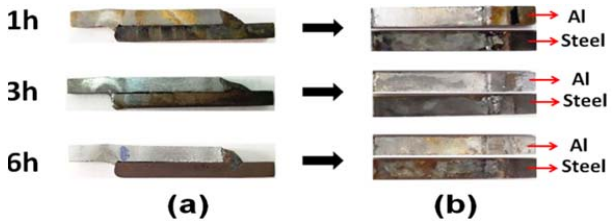

Fig. 1 (a) Outer surface of weld sample B1 after exposure to $FeCl_3$ solution for 1h, 3h and 6h (b) Inner surfaces of Aluminium and steel at the joint region showing their corrosion crevice behaviour

III. RESULTS AND DISCUSSION

Microscopy and corrosion analysis were carried out across various interfaces of the weld cross-section as shown in Fig. 2.

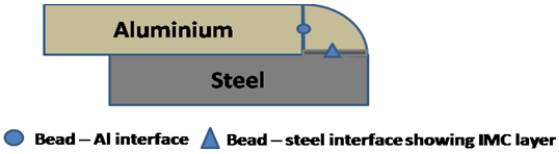

Fig. 2 Image of weld specimen showing interfaces

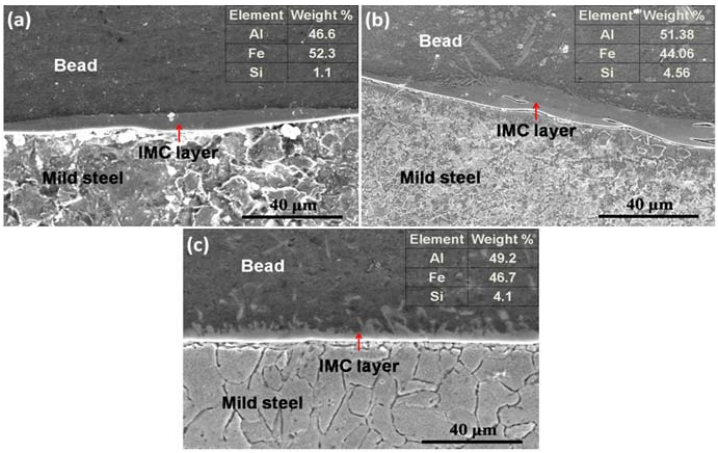

Fig. 3 SEM micrographs showing bead-steel interface in (a) sample B1, (b) B2 and (c) B3 with elemental analysis in the inset

A. Microstructural Analysis

1. Bead – Steel Interface

The work was initiated with fabrication of sample B1, setting the parameters for welding as per literature (weld speed: 0.9 m/min; wire feed rate: 4.5 m/min). An IMC layer width of 6.6 ± 0.9 µm was seen at the interface.

The wire feed rate was increased to 5.5 m/min in sample B2 which resulted in an increased layer width (8.2 ± 0.7 µm) proving that the layer width increases with the filler feed rate. This is because, increased feed rate of filler results in enhanced heat input (90.1 kJ/mm) leading to higher number of Aluminium atoms diffusing into Fe thereby, increasing the Al-Fe layer width. However, the layer width was found to decrease in sample B3 although the wire feed rate was higher (5 m/min). This is because of an increased weld speed in this sample (1 m/min). An increased weld speed contributes in decreased time for diffusion of Al in Fe of steel which lead to lowered layer width. The width was found to be 5.6 ± 0.11 µm in sample B3.

2. Elemental Analysis

The elemental analysis using EDX was done in the IMC layer area which confirmed the presence of elements Al and Fe. Moreover, higher weight percentage of Al was seen in the IMC layer of sample B2 (51.3 wt.%) than other samples which clearly proves the effect of high heat input during welding in the increased diffusion of Al into Fe of steel.

3. Bead – Al Interface

The micrographs at bead-Al interface remained similar to the three weld samples. The micrographs had shown mild grain coarsening at the interface because of high heat intensity in the fusion zone [19]. The EDX analysis at the interface had confirmed the generation of Al-Mg-Si precipitates in the three welds.

B. Micro XRD

The micro-XRD spectra of samples B1, B2 and B3 are shown in Fig. 5. From the figure, it is evident that the intermetallics such as Al_3FeSi_2, Al_5FeSi, $Fe_3Al_{0.7}Si_{0.3}$, $Fe_3Al_{0.5}Si_{0.5}$, FeAl and Fe_2Al_5 are formed in all the three samples. A high intensity Fe_2Al_5 peak is observed in the samples. Samples B1 and B2 have shown large number of intermetallics compared to sample B3. Zn was seen at low angles in samples B2 and B3 whereas in sample B1, it was observed at higher angles.

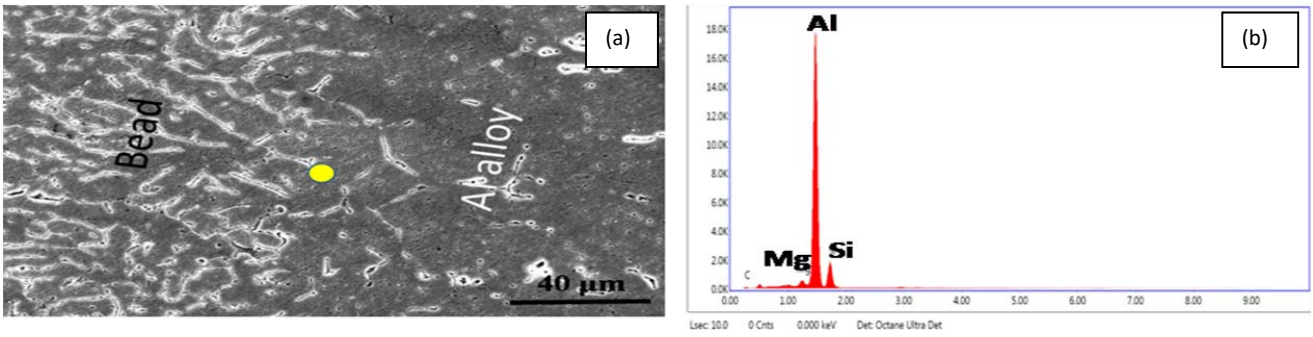

Fig. 4 Micrograph showing (a) bead-Al interface in sample B1; (b) EDX spectra of Al-Mg-Si precipitates at point indicated in (a)

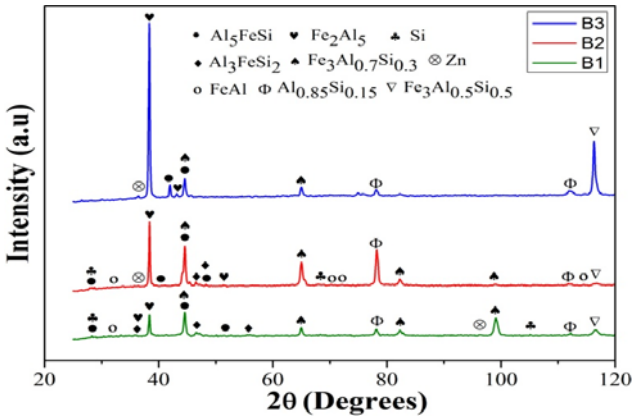

Fig. 5 Micro XRD patterns obtained in the IMC layer region of samples B1, B2 and B3

Al_5FeSi, FeAl and Si peaks were observed at lower angles in samples B1 and B2, but these compounds were found missing in sample B3. Similarly, $Fe_3Al_{0.7}Si_{0.3}$ intermetallics were observed at a diffraction angle of 98˚ in samples B1 and B2 whereas it was not observed in sample B3. Diffusion of Si from the filler to IMC layer, resulted in the generation of ternary Al-Fe-Si phases along with binary Al-Fe phases. The crystal structure of these phases is given in Table III.

TABLE III
CRYSTAL STRUCTURE OF THE PHASES FORMED IN THE IMC LAYER OF WELD SAMPLES [20]

Phases	Composition (atomic %)			Crystal structure
	Al	Fe	Si	
FeAl	50	50	--	Cubic
Fe_2Al_5	--	--	--	Orthorhombic
$Fe_3Al_{0.5}Si_{0.5}$	12.5	75	12.5	Cubic
$Fe_3Al_{0.7}Si_{0.3}$	17.5	75	7.5	Cubic
Al_5FeSi	71.43	14.29	14.29	Monoclinic
Al_3FeSi_2	50	16.67	33.33	Tetragonal

C. Corrosion Analysis

As the welds were in lap joint configuration, the interfacial gap between the joints was inevitable. The crevice corrosion

resistance of the joints was evaluated in high corrosive environment such 5 wt % $FeCl_3.6H_2O$ solution.

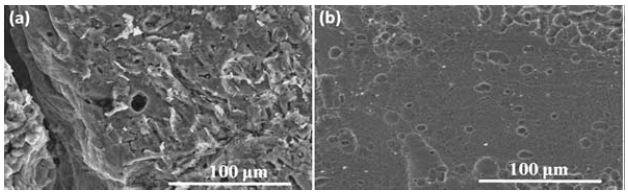

Fig. 6 Heavy oxidation taking place in (a) Aluminium and (b) Mild oxidation in Steel at the joint region due to exposure to $FeCl_3.6H_2O$ solution for 6 h

When the broken joints were examined, the inner surface of aluminium in sample B1 was evidenced with heavy oxidation at 6th hour ofexposing the welds to $FeCl_3$ solution. However, mild oxide cracking was observed on the surface of steel as shown in Fig. 6.

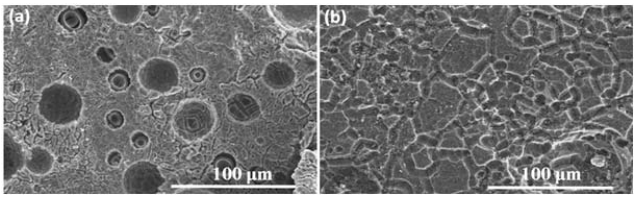

Fig 7 Heavy oxidation taking place in (a) Aluminium (b) Steel at the joint region of sample B2 due to exposure to $FeCl_3$ solution for 6 hours

The enhanced wire feed rate in sample B2 (5.5m/min) has increased the heat intensity (90 J/mm) during weld fabrication and this resulted in deterioration of crevice corrosion resistance in the weld sample B2. Consequently, both mild steel and Aluminium sides of the joint region were evidenced with heavy oxidation as shown in Fig. 7. Extensive pitting was observed on the aluminium side along with oxide cracking. The aluminium alloy was observed to corrode at a faster pace due to which the surface gradually started getting damaged.

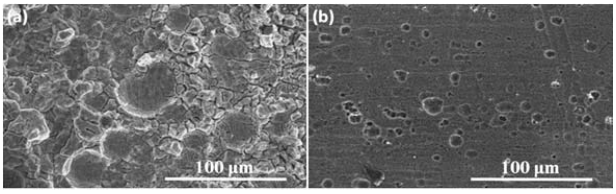

Fig. 8 Heavy oxidation taking place in (a) Aluminium and (b) Steel exhibiting pitting at the joint region of sample B3 due to exposure to $FeCl_3$ solution for 6 hours

The microstructures at the inner surfaces of sample B3 are given in Fig. 8. Similar to the previous samples, heavy oxidation was observed on the aluminium side of B3. However, mild pitting was observed on the steel side with no oxide cracking. This shows that the increased weld speed plays a major role in the enhancing the crevice corrosion resistance of mild steel.

1. Weight Loss Observations

Weight loss due to crevice corrosion in the weld samples was observed after carefully sectioning the joint region of the samples post $FeCl_3$ exposure. Clearly, sample B2 was found to exhibit greater weight loss (Table IV). The combinatorial effect of low weld speed and high filler feed rate has increased the IMC layer width which in turn deteriorated the corrosion resistance of B2 and lead to subsequent weight loss. However, careful optimization of filler feed rate and weld speed had reduced the weight loss in B2 due to lower IMC width. The weight loss was found to be lower in sample B1 although both aluminium and steel have exhibited low resistance to crevice corrosion.

TABLE IV
WEIGHT LOSS CALCULATIONS AFTER 1H, 3H AND 6H EXPOSURE TO $FECL_3.6H_2O$ SOLUTION OF WELD SAMPLES

Sample ID	Weight loss (mg)			Heat Input (J/mm)
	1h	3h	6h	
B1	10.4	28.7	27.4	80.9
B2	18.7	39.8	48.7	90.1
B3	13.03	29.3	44.4	85.3

IV. CONCLUSIONS

The MIG-braze joints of 6061 Al – Mild steel were fabricated in lap configuration at variant parameters. The following conclusions are obtained:

1) Although Al-Steel joints offer high mechanical strength in lap joint configuration, the interfacial gap resulting from these joints leads to crevice corrosion. However, this can be controlled by carefully optimizing the processing parameters.
2) Crevice corrosion in the weld joints increases with decreasing weld speed during welding.
3) Weight loss due to crevice corrosion is enhanced with increased heat input.
4) The diffusion of Si from the filler metal into the intermetallic layer resulted in the generation of Al-Fe-Si phases at the weld interface and this could be identified through phase analysis using micro-XRD technique.

REFERENCES

[1] H. Sakihama, H. Tokisue and K. Katoh, Mechanical Properties of Friction Surfaced 5052 Aluminum Alloy, Journal of Material Transactions, 2003, Volume: 44(12), p 2688-2694.
[2] H. Oikawa, T. Saito, T. Yoshimura, T. Nagase, T. Kiriyama, Spot welding of aluminium clad steel to steel or aluminium: Joining steel to aluminium with an intermediate layer, Japan Welding Society, 1996, Vol: 14, p 69-80.
[3] M. Kikuchi, H. Takeda, S. J. Morozumi, Friction Welding of Aluminium and Aluminium Alloys with Steel, Japan Institute of Light Metals, 1984, Vol: 34, p 165-173.
[4] SushovanBasak, Hrishikesh Das, Tapan Kumar Pal, Mahadev Shome, Characterization of intermetallics in aluminum to zinc-coated interstitial free steel joining by pulsed MIG brazing for automotive application, Journal of Material Characterization, 2016, Vol: 112, p 229–237.
[5] Hyoung Jin Park, Sehun Rhee, Mun Jin Kang and Dong Cheol Kim, Joining of Steel to Aluminium Alloy by AC Pulse MIG Welding, Journal of Material Transactions, 2009, Vol: 50(9), p 2314-2317.
[6] Yu Shi, Jie Li, Gang Zhang, Jiankang Huang, and Yufen Gu, Corrosion Behavior of Aluminum-Steel Weld-Brazing Joint, Journal of Materials Engineering and Performance, 2016, Vol: 25 (5), p 1916.

[7] Taban, E.; Kaluc, E.; Comparison between microstructure characteristics and joint performance of 5086-H32 aluminium alloy welded by MIG, TIG and friction stir welding processes, Journal of KovoveMaterialy, 2007, Vol: 45(5), p 241.

[8] Zhang, H. T.; Feng, J. C.; He, P.; Interfacial phenomena of cold metal transfer (CMT) welding of zinc coated steel and wrought aluminium, Journalof Materials Science and Technology. 2008, Vol: 24, p 1346-1349.

[9] Xiong J, Li J, Qian J, W, Zhang F., (2012) High strength lap joint of aluminium and stainless steels fabricated by friction stir welding with cutting pin", Science and Technology of Welding & Joining. Vol: 17(3), p 196-201, DOI: 10.1179/1362171811Y.0000000093

[10] Ahmed S, Abhishek, S, Akash, D., Saha, P, Shuja, A, (2014). Development and Analysis of Butt and Lap welds in Micro Friction Stir Welding (μFSW). Design and Research Conference, 5th International & 26th All India Manufacturing Technology, IIT Guwahati, Assam, India.

[11] Sravanthi S. S., Swati Ghosh Acharyya, Phani Prabhakar K. V.; Padmanabham G.; Effect of welding parameters on the corrosion behavior of dissimilar alloy welds of T6 AA6061 Al-Galvanized Mild Steel, Journal of Materials Engineering and Performance, 2018, Vol: 27(10), p 5518-5531, DOI: https://doi.org/10.1007/s11665-018-3596-z.

[12] Sravanthi S. S., Swati Ghosh Acharyya., Phani Prabhakar, K. V.; Padmanabham, G.; Integrity of 5052 Al-mild steel dissimilar welds fabricated using MIG-brazing and cold metal transfer in nitric acid medium, Journal of Materials Processing Technology, 2019, Vol: 268, p 97–106, DOI: https://doi.org/10.1016/j.jmatprotec.2019.01.010.

[13] Milani, A.; Paidar, M.; Khodabandeh, A.; Nategh, S.; Influence of filler wire and wire feed speed on metallurgical and mechanical properties of MIG welding–brazing of automotive galvanized steel/5754 aluminum alloy in a lap joint configuration, Journal of Advanced Manufacturing Technology. 2016, Vol: 82, p 1495–1506.

[14] Krishna P. Yagati, Ravi N. Bathe, Koteswararao V. Rajulapati, K. Bhanu Sankara Rao, G. Padmanabham, Fluxless arc weld-brazing of aluminum alloy to steel, Journal of Material Processing Technology, 2014, Vol: 214, p 2949–2959.

[15] Ali Mehrani Milani, Moslem Paidar, Alireza Khodabandeh, Saeed Nategh, Influence of filler wire and wire feed speed on metallurgical and mechanical properties of MIG welding–brazing of automotive galvanized steel/5754 aluminum alloy in a lap joint configuration, Journal of Advanced Manufacturing Technology, 2016, Vol: 82, p 1495–1506.

[16] Padmanabham, G., Krishna Priya, Y., Phani Prabhakar, K. V., Ravi N., Bathe, BhanuSankara Rao, K. A comparison of interface characteristics and mechanical properties of aluminium-steel joints made by P-MIG and cold metal transfer (CMT) processes. In: Trends in Welding Research: Proceedings of 9th International Conference, 2013, p 227–234.

[17] Cullity, B. D.; Elements of X-Ray diffraction, 3rd ed., Prentice Hall, 2001.

[18] Standard Test Methods for Pitting and Crevice Corrosion Resistance of Stainless Steels and Related Alloys by Use of Ferric Chloride Solution, ASTM G 48-03, American Society for Testing and Materials, 2002.

[19] Wan S., Muda H. W., Nurul S., Nasir M., Effect of welding heat input on microstructure and mechanical properties at coarse grain heat affected zone of ABS grade a steel, ARPN Journal of Engineering and Applied Sciences,2016, Vol:10(15), ISSN 1819-6608.

[20] Y. Li, B. Legendre, Enthalpy of formation of Al–Fe–Si alloys II, Journal of Alloys and Compounds, 2000, Vol: 302, p 187-191.

[21] S. S. Sravanthi, Swati Ghosh Acharyya, K.V. Phani Prabhakar, Joydip Joardar, "Effect of varying weld speed on the corrosion resistance and mechanical behaviour of Aluminium – Steel Welds fabricated by Cold Metal Transfer Technique", Journal of Materials and Manufacturing Process, https://doi.org/10.1080/10426914.2019.1605180.